P
2mif

NASA CR-134545
BCAC D6-41499

THE RESULTS OF A HIGH-SPEED WIND TUNNEL TEST TO INVESTIGATE THE EFFECTS OF THE NASA REFAN JT8D ENGINE NACELLES ON THE STABILITY AND CONTROL CHARACTERISTICS OF THE BOEING 727 AIRPLANE

by E. A. Kupcis

BOEING COMMERCIAL AIRPLANE COMPANY
A DIVISION OF
THE BOEING COMPANY

Prepared for

NATIONAL AERONAUTICS AND SPACE ADMINISTRATION

NASA Lewis Research Center

Contract NAS3-17842

1. Report No.	2. Government Accession No.	3. Recipient's Catalog No.
CR-134545		

4. Title and Subtitle	5. Report Date
The Results of a High-Speed Wind Tunnel Test to Investigate the Effects of the NASA Refan JT8D Engine Nacelles on the Stability and Control Characteristics of the Boeing 727 Airplane,	December 1973
	6. Performing Organization Code
7. Author(s)	8. Performing Organization Report No.
E. A. Kupcis	D6-41499
	10. Work Unit No.
9. Performing Organization Name and Address	11. Contract or Grant No.
Boeing Commercial Airplane Company P. O. Box 3707 Seattle, Washington 98124	NAS3-17842
12. Sponsoring Agency Name and Address	13. Type of Report and Period Covered
National Aeronautics and Space Administration Washington, D. C. 20546	Contractor Report
	14. Sponsoring Agency Code

15. Supplementary Notes

Project Manager, A. A. Medeiros
NASA Lewis Research Center, Cleveland, Ohio 44135

16. Abstract

A high speed wind tunnel test was conducted to investigate the effects of the NASA Refan JT8D engine nacelles on the stability and control characteristics of the Boeing 727 airplane. The test was performed at the Calspan Corporation 8x8 ft. (2.44x2.44 m.) transonic wind tunnel. It was conducted by the Flight Controls Technology Staff of the Boeing Commercial Airplane Company in support of NASA Contract NAS 3-17842, "Phase II Program on Ground Test of Refanned JT8D Turbofan Engines and Nacelles for the 727 Airplane." Both the 727-200 and -100 models were tested. A small nose-down pitching moment increment and a slight increase in longitudinal stability were noted due to the Refan nacelles. The directional stability of the 727-200 airplane increased up to 10 percent. A smaller improvement was observed on the 727-100 model. In general, the high speed stability and control characteristics of the basic airplane are not significantly altered by the Refan nacelle installation.

17. Key Words (Suggested by Author(s))	18. Distribution Statement
Boeing 727 NASA Refan Nacelles Wind Tunnel High Speed Longitudinal Stability and Control Lateral-Directional Stability and Control	Unclassified - Unlimited

19. Security Classif. (of this report)	20. Security Classif. (of this page)	21. No. of Pages	22. Price*
Unclassified	Unclassified		

* For sale by the National Technical Information Service, Springfield, Virginia 22151

FOREWORD

The high-speed wind tunnel test described in this report was performed by the Flight Controls Technology Staff of the Boeing Commercial Airplane Company, a division of The Boeing Company, Seattle, Washington. The work, sponsored by NASA Lewis Research Center and reported herein, was performed in October 1973.

This report has been reviewed and is approved by:

F. C. Hall — Date 2.4.74
F. C. Hall, Group Engineer
Flight Controls Technology Staff

J. A. Ferrell — Date 2.4.74
J. A. Ferrell
Chief, Staff Technology
JT8D Refan Program

K. P. Rice — Date 2/4/4
K. P. Rice
Program Manager
JT8D Refan Program

TABLE OF CONTENTS

1.0 SUMMARY

A high-speed wind tunnel model of the Boeing 727 airplane was tested in support of the NASA Refan program. The purpose of the test was to investigate the effects of the larger Refan nacelles on the longitudinal and lateral-directional stability and control characteristics of the 727 airplane.

The following conclusions are made:

1. The effect of NASA Refan nacelles on the high-speed longitudinal stability and control characteristics of the 727-200 and -100 airplanes is minor. A small nose down pitching moment increment and a slight increase in longitudinal stability was noted.

2. Directional stability (C_{n_β}) of the 727-200 airplane increased up to 10% due to installation of the Refan nacelles. A smaller improvement was noted on the 727-100 model.

3. In general, the high-speed stability and control characteristics of the 727 Refan airplane are very similar to those of the Basic 727.

2.0 INTRODUCTION

The Pratt & Whitney Aircraft JT8D-109 engine is a derivative of the basic JT8D-9 turbofan engine, modified to incorporate a new, larger diameter, single-stage fan with a bypass ratio of 2.03 and two supercharging low-pressure compressor stages. The modification gives lower jet noise, increased takeoff and cruise thrust, and lower specific fuel consumption. The use of the JT8D-109 engine on the Boeing 727 airplane will require enlarged side engine nacelles and center engine inlet, referred to as the NASA Refan Configuration.

Previous wind tunnel testing has shown that aft body mounted nacelles on a T-tail transport can have a significant effect on the longitudinal and lateral-directional stability and control characteristics. This effect consists of two parts: aerodynamic forces on the nacelle itself and interference effects between the nacelles and the empennage. The relative magnitude of the effect is a function of nacelle size and the location of the nacelle relative to the vertical and horizontal tails, the body, and wing.

In the pitch axis, larger nacelles tend to increase the stability at low angles of attack. At high, post-stall α's the increased interference tends to reduce stabilizer and elevator effectiveness. Stability changes at high Mach number due to larger nacelles could adversely affect high speed tuck characteristics.

In the yaw axis, larger side nacelles reduce vertical tail effectiveness due to increased aerodynamic interference. This has an adverse effect on airplane Dutch roll characteristics.

Due to the complex nature of these effects, wind tunnel testing was required to determine the influence of the larger NASA Refan nacelles on the stability and control characteristics of the 727 airplane.

Low-speed wind tunnel tests were conducted at the Boeing Vertol Wind Tunnel (May and June 1973) and at the University of Washington Aeronautical Laboratory (August 1973). The results of these tests are reported in Reference 1. Among the items investigated was the effect of side nacelle location on post-stall high angle of attack pitch characteristics. The most favorable location for the Refan nacelle was found to be the production JT8D-9 nacelle location.

High-speed longitudinal and lateral-directional stability and control characteristics of the NASA Refan 727 airplane were evaluated in the Calspan Corporation, 8x8 ft. (2.44x2.44 meter) transonic wind tunnel in October 1973. The Refan side nacelle location, as determined from the low-speed testing, was used. Both the 727-200 and -100 airplanes were evaluated.

The effect of the Refan nacelles on the high-speed stability and control characteristics of the 727 airplane as determined from the Calspan test is the subject of this report. The emphasis is on the 727-200 results, although some -100 data are also given. Since high-speed aeroelastic corrections have a considerable effect on all of the data shown, it should not be used for absolute performance levels, but is intended only to provide an increment between the basic and Refan 727 configurations.

3.0 NOMENCLATURE

a.c.	Aerodynamic center (neutral point), percent MAC
b	Wing span
$\bar{c}$	Mean aerodynamic chord of the wing
C_L	Airplane lift coefficient, lift/qS_w, positive up
$C_{M.25}$	Pitching moment coefficient about the quarter MAC, pitching moment/$qS_w\bar{c}$, positive airplane nose up.
C_{M_Δ}	Variation of pitching moment with horizontal stabilizer incidence angle, $\partial C_M / \partial \Delta_{wcp}$
C_n	Yawing moment coefficient about the quarter MAC, Yawing moment/qS_wb, positive airplane nose right.
C_{n_β}	Variation of yawing moment with sideslip angle, $\partial C_n / \partial \beta$
C_l	Rolling moment coefficient, rolling moment/qS_wb, positive right wing down.
C_{l_β}	Variation of rolling moment with sideslip angle, $\partial C_l / \partial \beta$
C_y	Side force coefficient, side force/qS_w, positive right
C_{y_β}	Variation of side force with sideslip angle, $\partial C_y / \partial \beta$
D_{HI}	Nacelle hilite diameter
$D_{max.}$	Nacelle maximum diameter
D_N	Nozzle exit diameter
D_{TH}	Nacelle throat diameter
M	Mach number
MAC	Mean Aerodynamic Chord

N/m^2	Pressure in Newtons per square meter
psf	Pressure in pounds per square foot
q	Freestream dynamic pressure
i_{wcp}	Horizontal stabilizer incidence relative to the wing chord plane, degrees, positive trailing edge down
S_W	Wing reference area
wcp	Wing chord plane
X	Length to maximum nacelle section
α	Angle of attack, degrees
α_{wcp}	Wing angle of attack, degrees
β	Angle of sideslip, degrees, positive for wind from right.
θ	Nacelle boattail angle, degrees.

4.0 MODEL AND TEST DESCRIPTION

4.1 MODEL DESCRIPTION

4.1.1 BASIC MODEL

The model, designated TX-509I-10, is a 4.6 percent scale model of the Boeing 727 airplane. Two, 10 foot (3.05 meter), constant section body inserts, one forward and the other aft of the wing, were used to permit testing both the 727-100 and -200 configurations. A three-view drawing of the 727-200 NASA Refan configuration indicating the major dimensions is shown in Figure 1. The model was sting mounted with an internal, six-component, strain gauge balance for measuring forces and moments. The basic model was modified to accept the NASA Refan side nacelles and center engine inlet. Trip strips on the wing, horizontal and vertical tail were used to simulate full scale boundary layer conditions. The model installation and a close-up view of the Refan nacelles are shown in Figures 2 and 3 respectively.

4.1.2 NACELLE GEOMETRY

The JT8D-109 NASA Refan engine requires a larger nacelle due to its higher bypass ratio. The geometry of the NASA Refan and the basic 727 nacelles as tested is shown in Figure 4. The side nacelles were of the flow-through type and the center engine inlet was plugged. The exit diameter of the side nacelles tested was enlarged from that of the actual nacelles to more correctly simulate the inlet flow field and its interaction with the empennage.

A plugged center engine inlet configuration was tested since the sting mount precluded the use of a flow-through design. Previous wind tunnel testing has shown the effects of the inlet plug to be negligible in both pitch and yaw.

4.2 TEST FACILITY AND MODEL INSTALLATION

The test was conducted at the Calspan Corporation transonic wind tunnel in Buffalo, N.Y. The test facility has a square 8x8 foot (2.44x2.44 meter) perforated wall test section, and is pressurized. However, this test was run at a total pressure of 1 atmosphere for all Mach numbers. At M = .95, the maximum Mach number tested, dynamic pressure was 750 psf (35,850 N/m^2) and Reynolds number per foot was 4.0×10^6 (13.1×10^6 per meter).

The model was installed on the Boeing 635H, six-component, internal strain gauge balance. The Calspan Corporation double-roll sting strut mechanism was used. This installation permitted pitch and yaw run combinations to be made without the necessity of a model change and tunnel shut down.

4.3 TEST PROCEDURE

The Mach number test range was 0.40 to 0.95 (some tail-off data were obtained up to M=0.90 only). The angle of attack pitch series was from -1° to +12° at low Mach number, with a lower α limit at high Mach number. The model was yawed between limits of ± 5 degrees at constant angle of attack (0.2°, 2.2° and 4.2°). Six-component force and moment data were recorded and standard wind tunnel corrections applied. Data repeatability was considered good.

PRECEDING PAGE BLANK NOT FILMED

5.0 DISCUSSION OF TEST RESULTS

5.1 LONGITUDINAL CHARACTERISTICS

The effect of NASA Refan nacelles on the longitudinal stability and control characteristics of the 727 airplane is shown in Figures 5 to 11. Data plots of lift coefficient (C_L) versus pitching moment coefficient about the quarter MAC ($C_{M.25}$) are given for Mach numbers of 0.40, 0.80, 0.85 and 0.90 for the 727-200 airplane (Figures 5 to 8), and at M = 0.40 and 0.85 for the 727-100 model (Figures 9 and 10). Horizontal tail on and off data are shown for the -200 airplane while only tail on data are available for the -100.

The most apparent effect of the Refan nacelles on the 727-200 model is a nose down pitching moment increment. This increment occurs for both the horizontal tail on and off configurations, and it exhibits a typical Mach variation; increasing in magnitude with Mach number. The effect on airplane trim characteristics is expected to be minor.

In addition, the 727-200 Refan configuration shows a small increase in longitudinal static stability (Figure 11). Aft movement of the aerodynamic center occurs for both the tail off and on configurations. The increase in stability is a function of Mach number and varies from 4% MAC to no effect at all. The pitch characteristics at stall C_L's are also slightly improved for the Refan configuration.

Analysis of the horizontal tail on data for the 727-200 model indicates a small decrease in horizontal tail effectiveness ($C_{M_{i}}$) for the Refan airplane. The apparent change in $C_{M_{i}}$ is not considered significant since it falls within the data scatter band from previous wind tunnel tests conducted on the basic 727 airplane.

The effect of the Refan nacelles on 727-100 airplane longitudinal characteristics (Figures 9 and 10) is similar to that of the 727-200 airplane. There is a nose down pitching moment increment due to the Refan nacelles, with a slight increase in longitudinal stability. For the data at a tail incidence of -4 degrees, the nose down pitching moment increment does not appear. It is suspected that this is due to a discrepancy in the tail incidence setting.

The Refan nacelle effect on airplane lift coefficient is small. Representative data at a Mach number of 0.85 are shown in Figure 12 for the 727-200 airplane.

5.2 LATERAL-DIRECTIONAL CHARACTERISTICS

The effect of the NASA Refan nacelles on 727 airplane lateral-directional stability is shown in Figures 13 to 20. Stability derivatives C_{n_β} , C_{l_β} and C_{Y_β} are shown plotted versus Mach number. The basic airplane and Refan configurations are compared at wing angles of attack of α_{wcp} = 0.2°, 2.2° and 4.2°. The 727-200 airplane data (Figures 13 to 16) include vertical tail on and off data for both the Refan and basic airplanes. For the 727-100 model (Figures 17 to 20) vertical tail on data are given for both configurations, but vertical tail off data are available only for the Refan configuration.

The stability derivatives were calculated from plots of C_n, C_l and C_y versus β ; typical examples of which are shown in Figures 21 to 23. The data are for the 727-200 basic and Refan airplanes at a Mach number of 0.85 and $\alpha_{wcp} = 2.2°$. Slopes were taken over a β range of ± 1 degree. However, data linearity is quite good, and the derivatives can generally be used up to sideslip angles of ± 2 degrees.

Figure 13 indicates a 10% increase in directional stability ($C_{n\beta}$) due to the Refan nacelles for the 727-200 airplane over the Mach number range 0.40 to 0.85. At Mach numbers greater than 0.85, the nacelle effect is smaller. Past wind tunnel data on derivative 727 airplanes indicate that larger side nacelles are destabilizing. The larger Refan center engine inlet provides enough added directional stability to offset the destabilizing effect of the Refan side nacelles and actually results in a net gain in stability. As seen in Figure 13, with the vertical tail off (including the center engine inlet and horizontal tail), the Refan nacelles have very little effect on $C_{n\beta}$.

The lateral stability derivative $C_{l\beta}$ and side force derivative $C_{Y\beta}$ for the 727-200 airplane (Figures 14 to 16) exhibit trends which are consistent with the observed increase in $C_{n\beta}$. Vertical tail on $C_{l\beta}$ and $C_{Y\beta}$ are larger for the Refan configuration at the lower Mach numbers, with the vertical tail off data showing very little effect of Refan nacelles.

Refan nacelle effects on 727-100 lateral-directional stability are shown in Figures 17 to 20. The data indicate a slight increase in directional stability ($C_{n\beta}$) at low Mach number due to the Refan nacelles. However, the effect is not as large or as well defined as that for the 727-200 airplane. $C_{l\beta}$ is essentially identical for the basic and Refan configurations. The increase in $C_{Y\beta}$ at low Mach number is very similar to that seen on the 727-200.

The effect of the Refan nacelles on the 727-100 airplane is less pronounced than on the -200 due to the shorter tail arm of the former. The side force ($C_{Y\beta}$) increment is essentially the same for both airplanes, whereas the Refan effect on moments is substantially less on the -100 airplane.

6.0 CONCLUSIONS

The effects of installing the P&W JT8D-109 NASA Refan nacelles on the Boeing 727 airplane were investigated in a high-speed wind tunnel test. Longitudinal and lateral-directional stability and control characteristics of the 727-200 and -100 models were evaluated.

Refan nacelle effects on longitudinal stability and control characteristics for both the 727-200 and -100 airplanes were found to be small. The nacelles cause a small nose down pitching moment and a slight increase in static stability.

727-200 airplane directional stability ($C_{n\beta}$) increased up to 10% due to installation of the Refan nacelles. This increase is attributed primarily to the larger side area of the Refan center engine inlet. The 727-100 model showed only a slight increase in $C_{n\beta}$ due to the Refan nacelles. The nacelle effect on the roll and side force derivatives, $C_{l\beta}$ & $C_{Y\beta}$ followed the same trend as that observed for $C_{n\beta}$.

In general, the high-speed stability and control characteristics of the basic and Refan 727 airplanes are very similar.

7.0 REFERENCES

1. M. D. Shirkey, "The Results of Low-Speed Wind Tunnel Tests to Investigate the Effects of the NASA Refan JT8D Engine Nacelles on the Stability and Control Characteristics of the Boeing 727-200." NASA CR-134503, October 1973.

PRECEDING PAGE BLANK NOT FILMED

8.0 LIST OF FIGURES

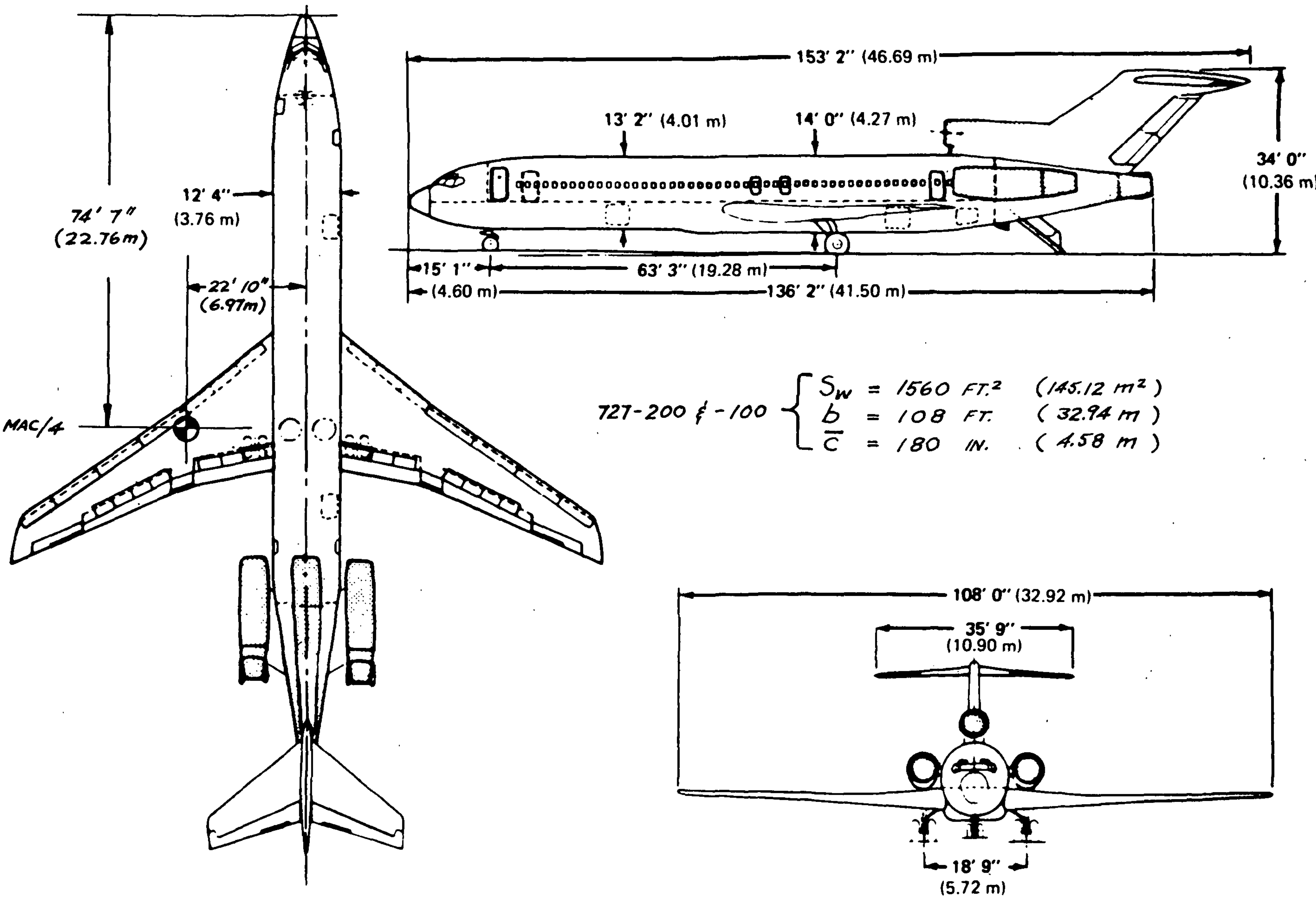

FIGURE 1.–727-200/JT8D-109 NASA REFAN AIRPLANE

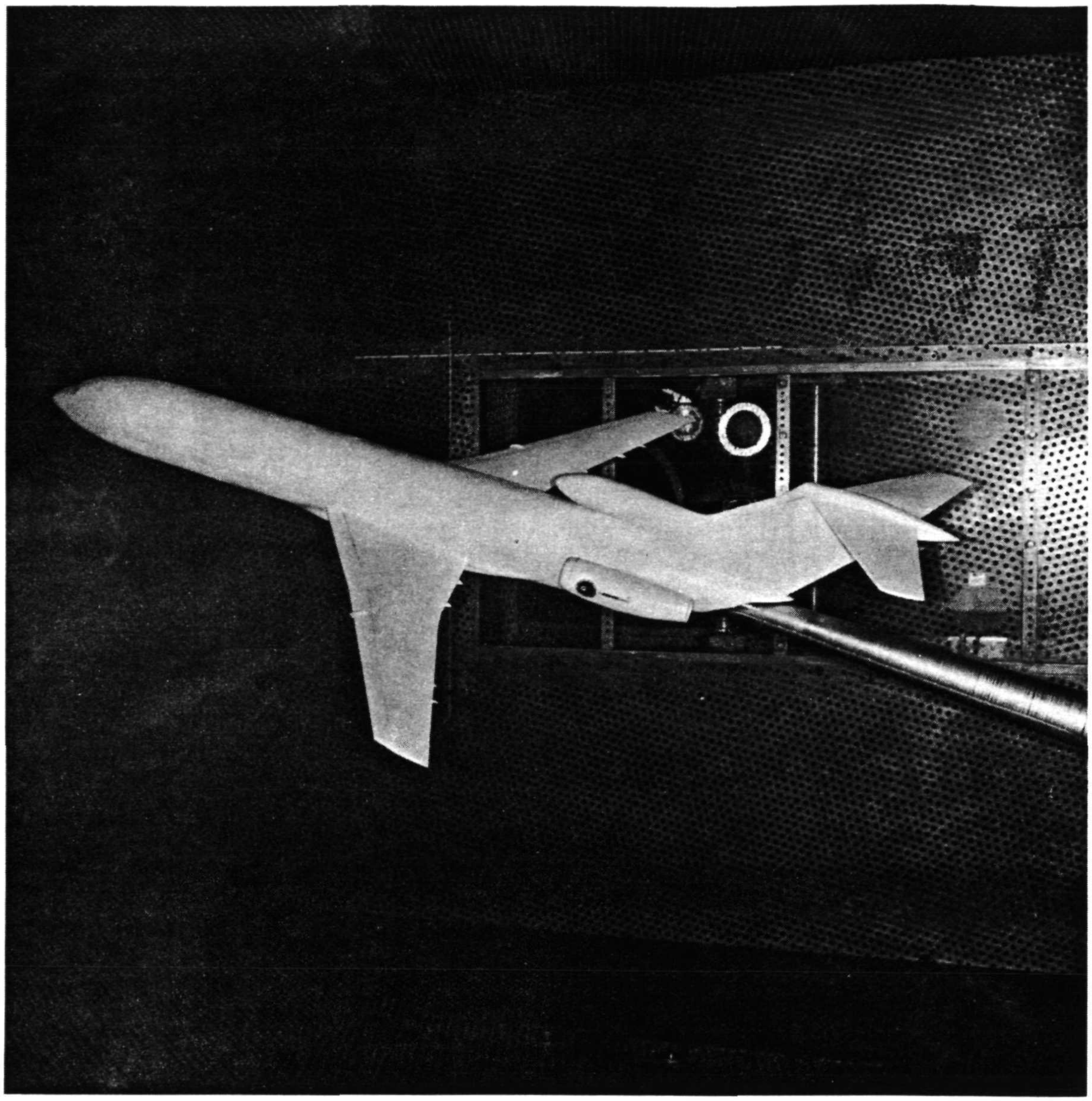

FIGURE 2.—727-200/JT8D-109 NASA REFAN MODEL INSTALLED IN THE CALSPAN CORPORATION TRANSONIC WIND TUNNEL

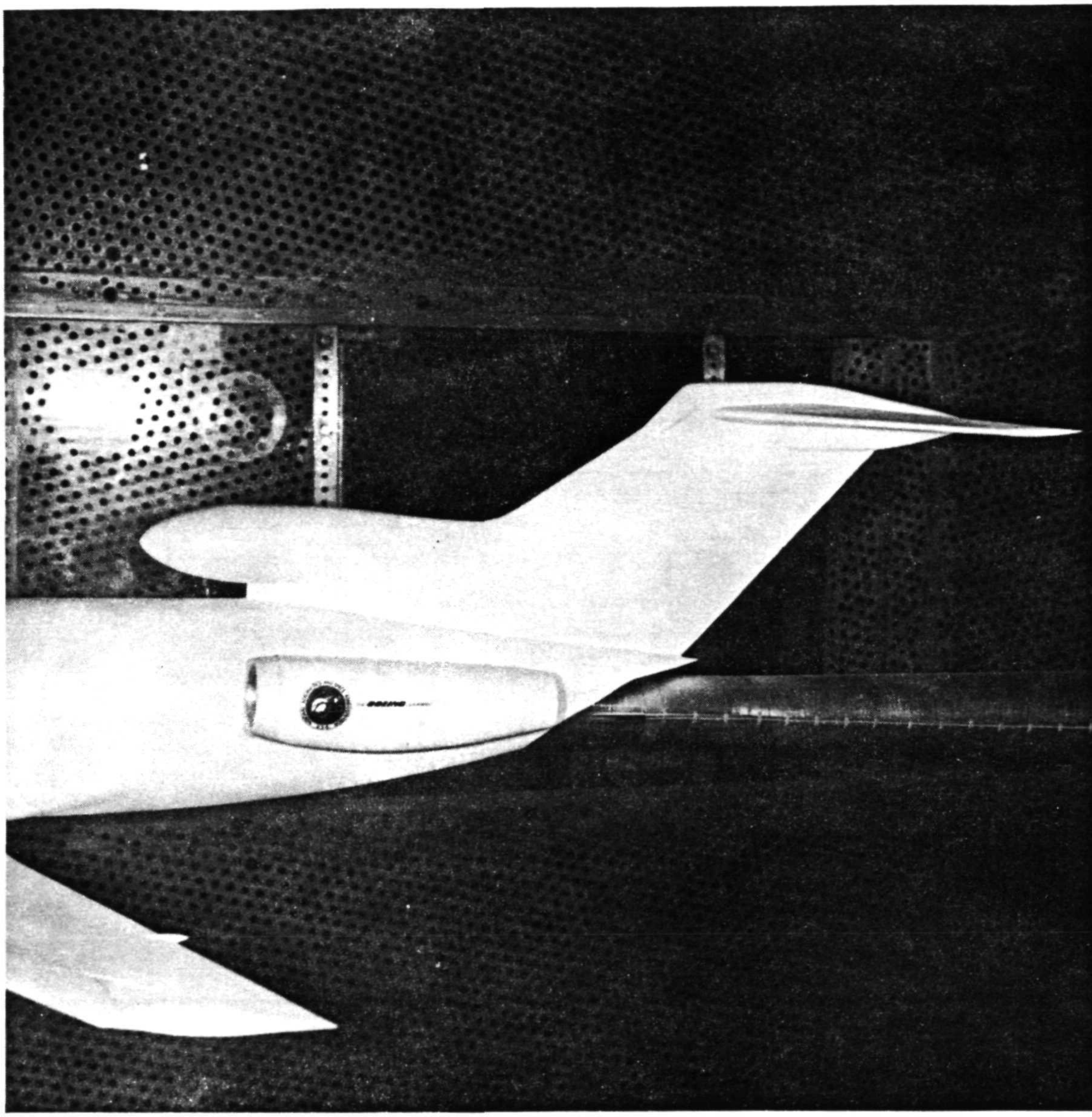

FIGURE 3.—727-200/JT8D-109 NASA REFAN NACELLE INSTALLATION

NACELLE PLAN VIEW

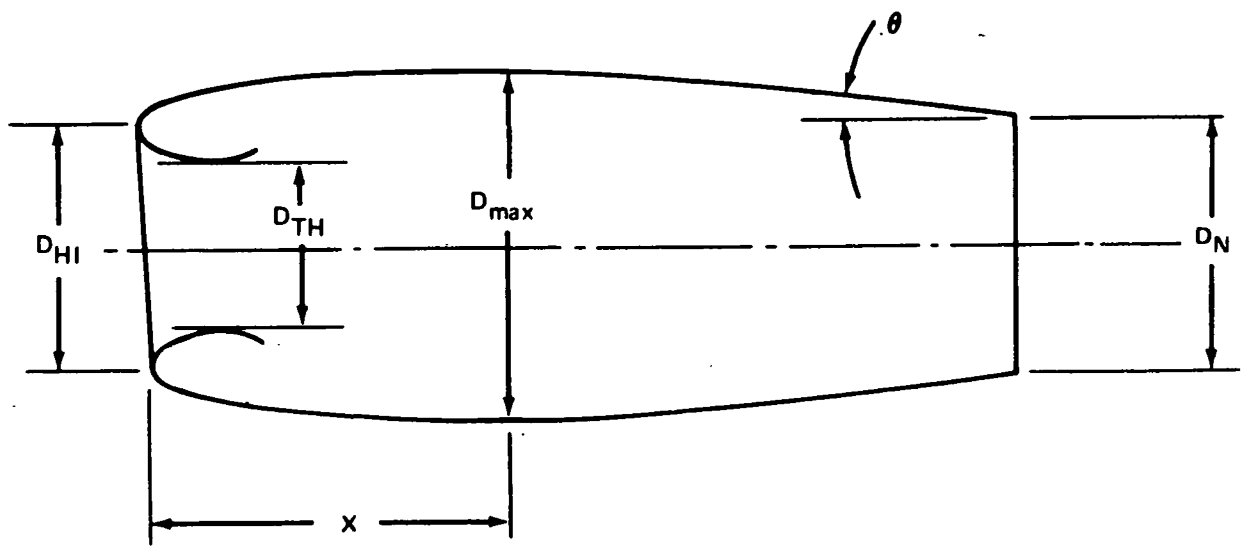

	Production side nacelle JT8D-9	NASA refan side nacelle JT8D-109	Production center inlet JT8D-9	NASA refan center inlet JT8D-109
Nacelle length, in. (cm)	188.2 (478.0)	233.1 (592.1)	—	—
Maximum diameter, D_{max}, in. (cm)	51.0 (129.5)	62.0 (157.5)	51.0 (129.5)	64.8 (164.6)
Nozzle exit diameter, D_N, in. (cm)	34.1 (86.6)	43.0 (109.2)	PLUGGED	PLUGGED
Length to maximum section, X, in.(cm)	30.0 (76.2)	33.5 (85.1)	32.6 (82.8)	34.9 (88.6)
Throat diameter, D_{TH}, in. (cm)	38.0 (96.5)	46.7 (118.6)	PLUGGED	PLUGGED
Hilite diameter, D_{HI}, in. (cm)	42.0 (106.7)	52.2 (132.6)	PLUGGED	PLUGGED
Tail pipe boattail angle, θ, deg (rad)	8.5 (0.148)	10.1 (0.176)	—	—

FIGURE 4.—NACELLE GEOMETRY AS TESTED

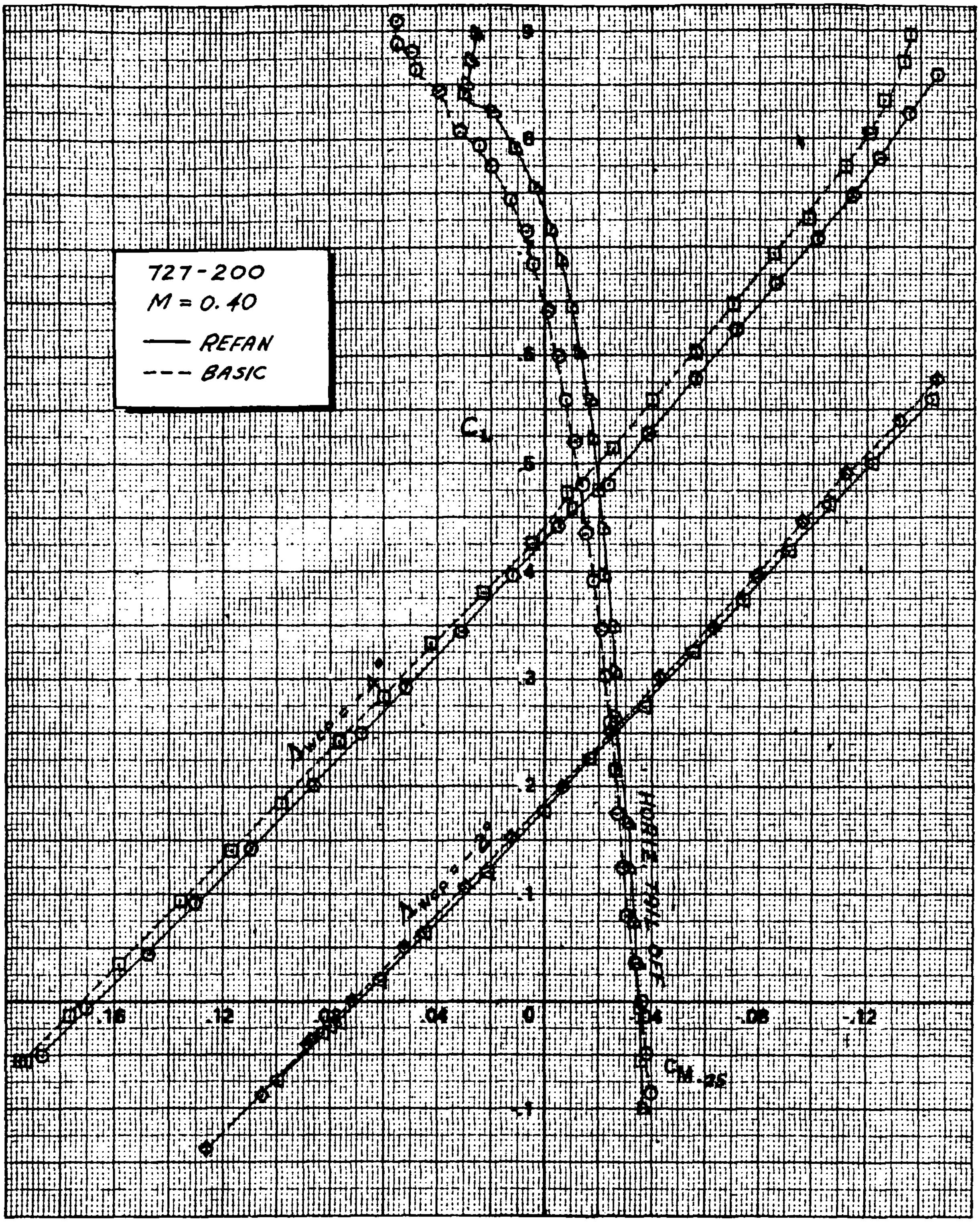

FIGURE 5. — EFFECT OF NASA REFAN NACELLES ON PITCHING MOMENT, 727-200, M = 0.40

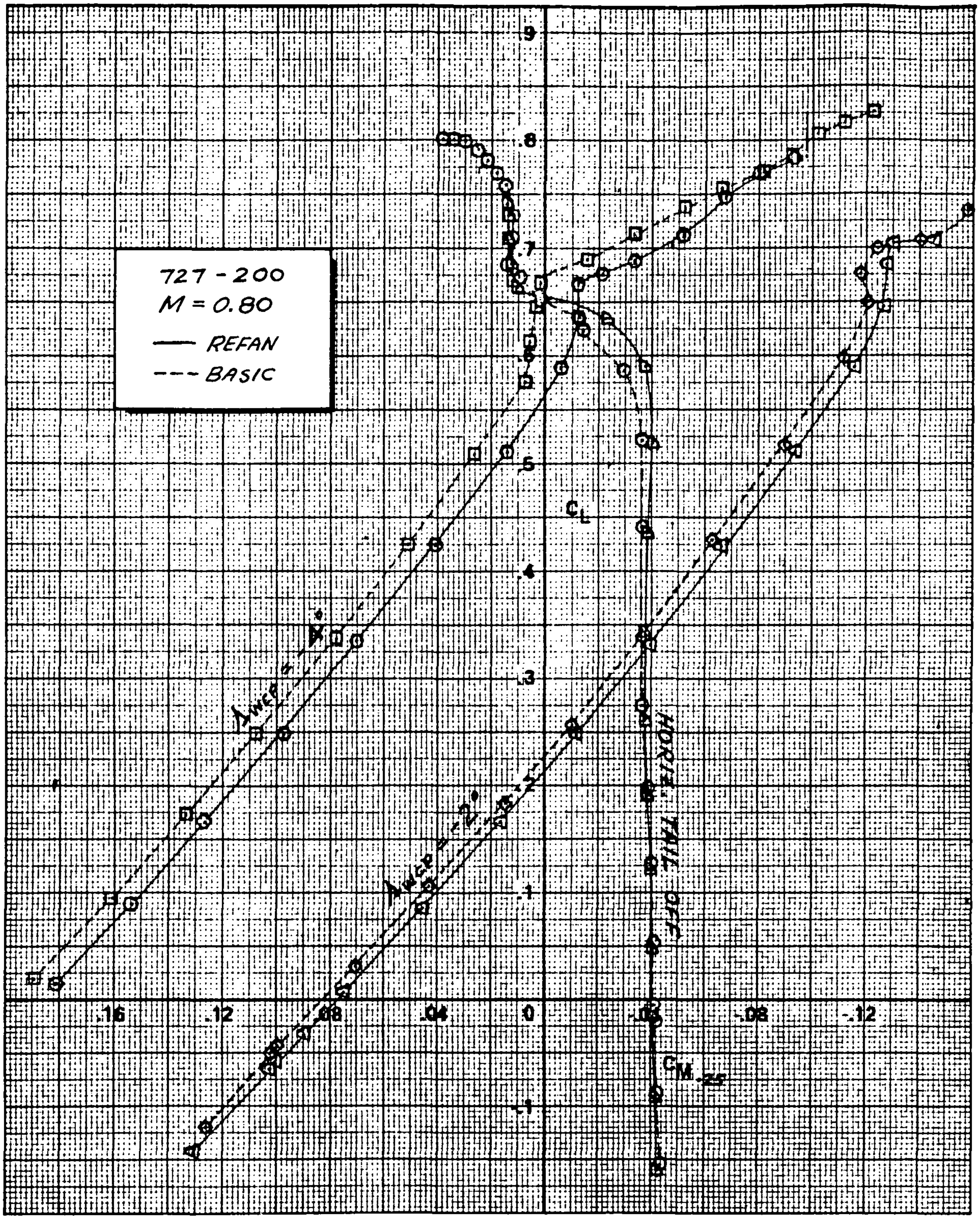

FIGURE 6. – EFFECT OF NASA REFAN NACELLES ON PITCHING MOMENT, 727-200, M = 0.80

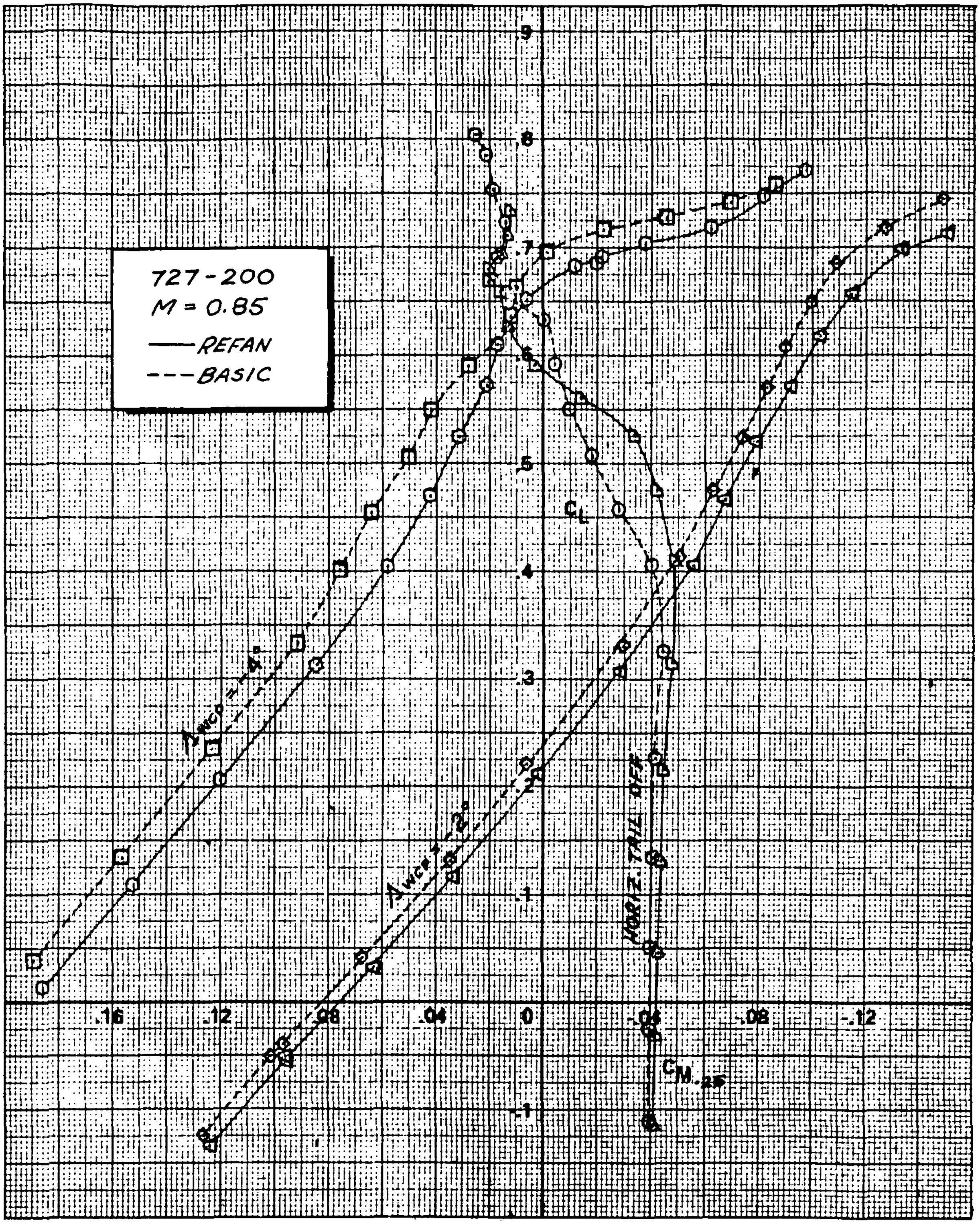

FIGURE 7. – EFFECT OF NASA REFAN NACELLES ON PITCHING MOMENT, 727-200, M=0.85

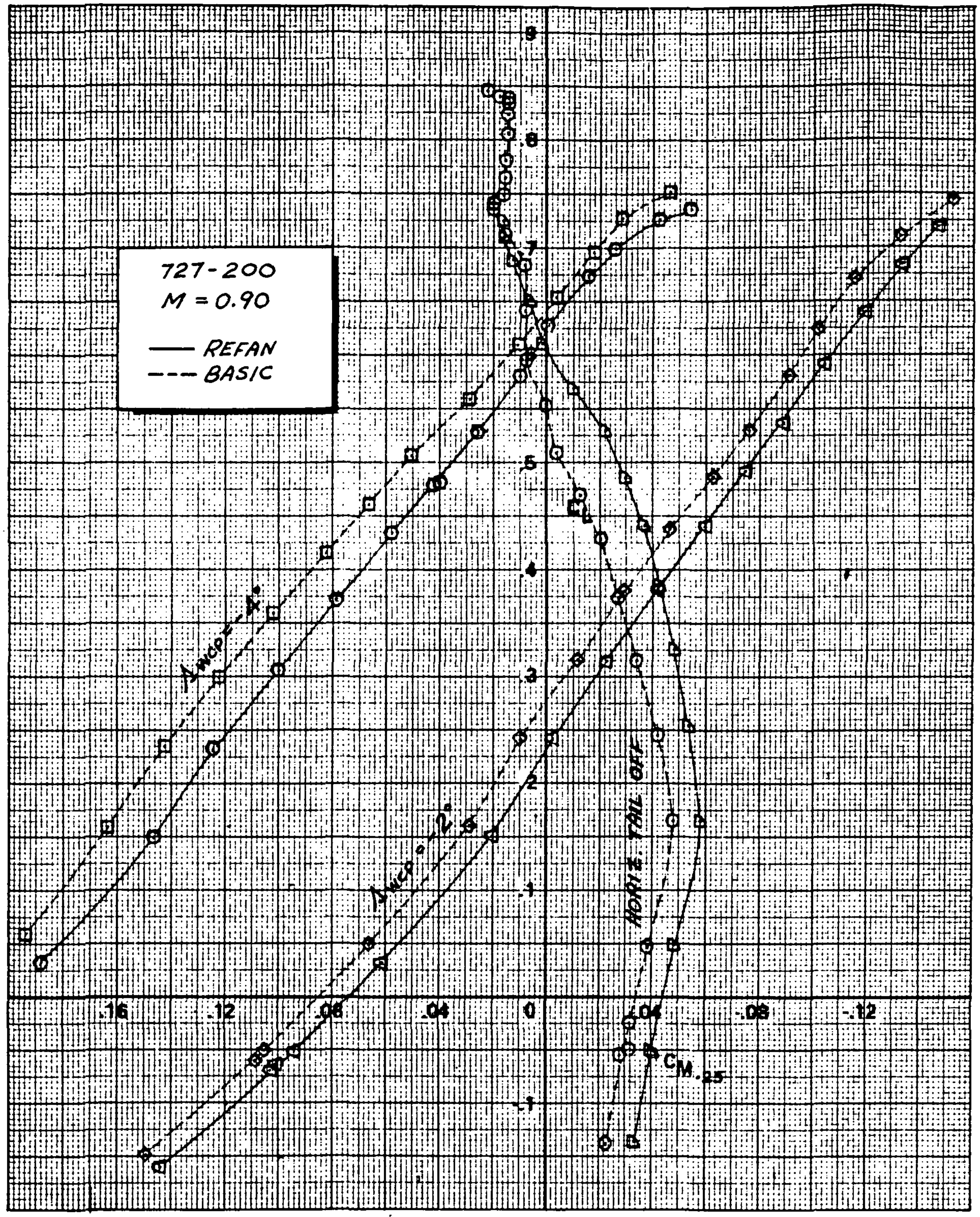

FIGURE 8. – EFFECT OF NASA REFAN NACELLES ON PITCHING MOMENT, 727-200, M = 0.90

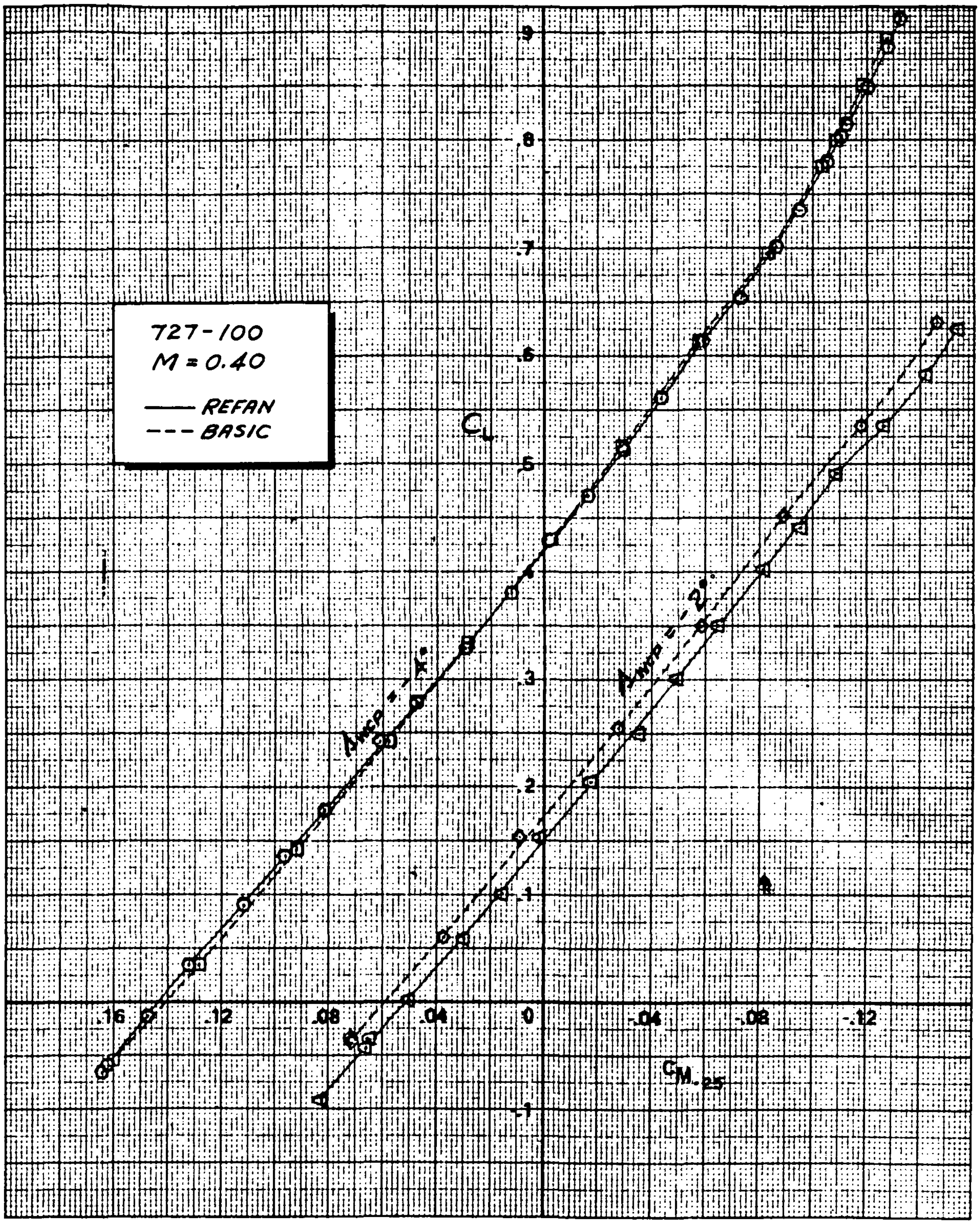

FIGURE 9. - EFFECT OF NASA REFAN NACELLES ON PITCHING MOMENT, 727-100, M = 0.40

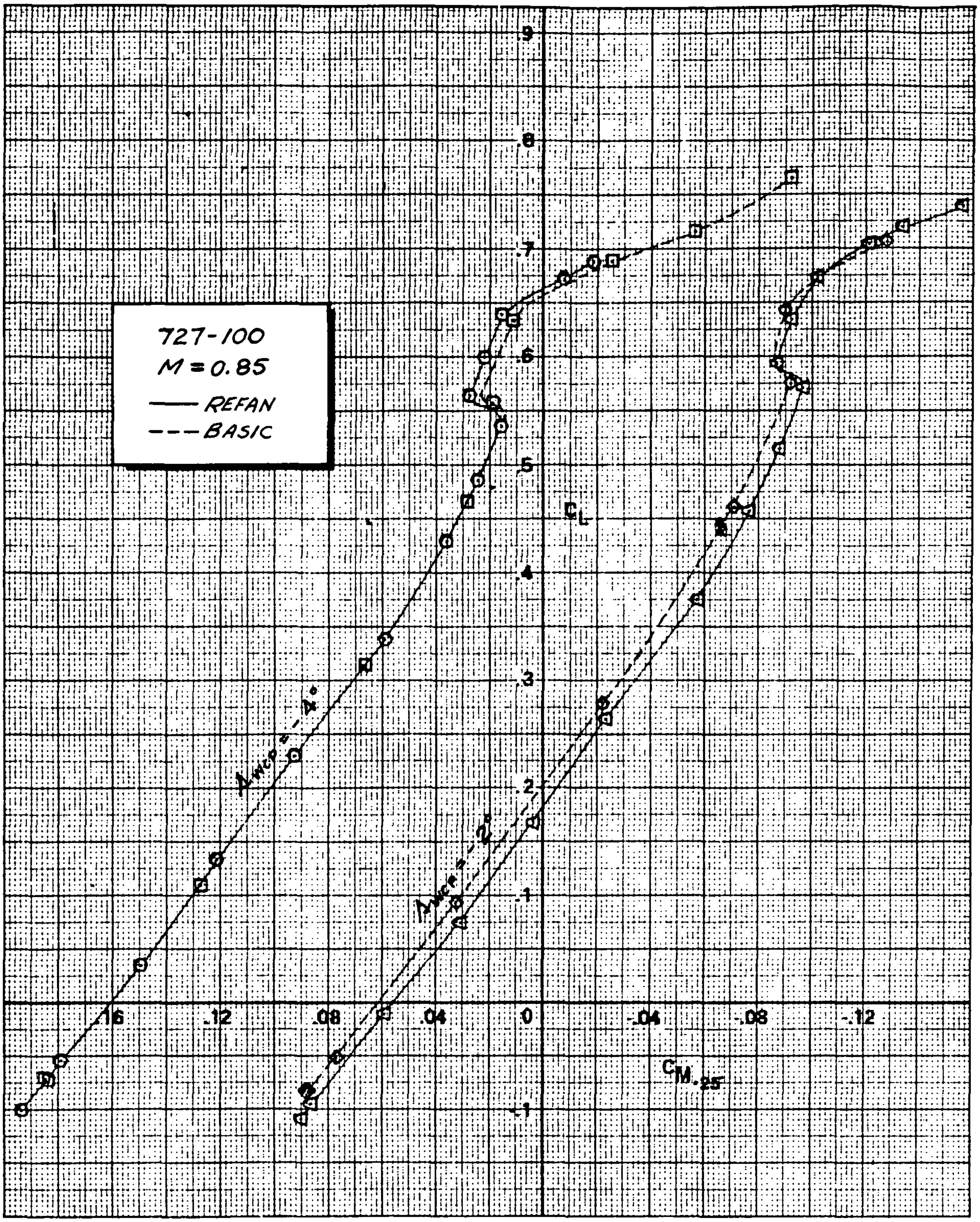

FIGURE 10. – EFFECT OF NASA REFAN NACELLES ON PITCHING MOMENT, 727-100, M = 0.85

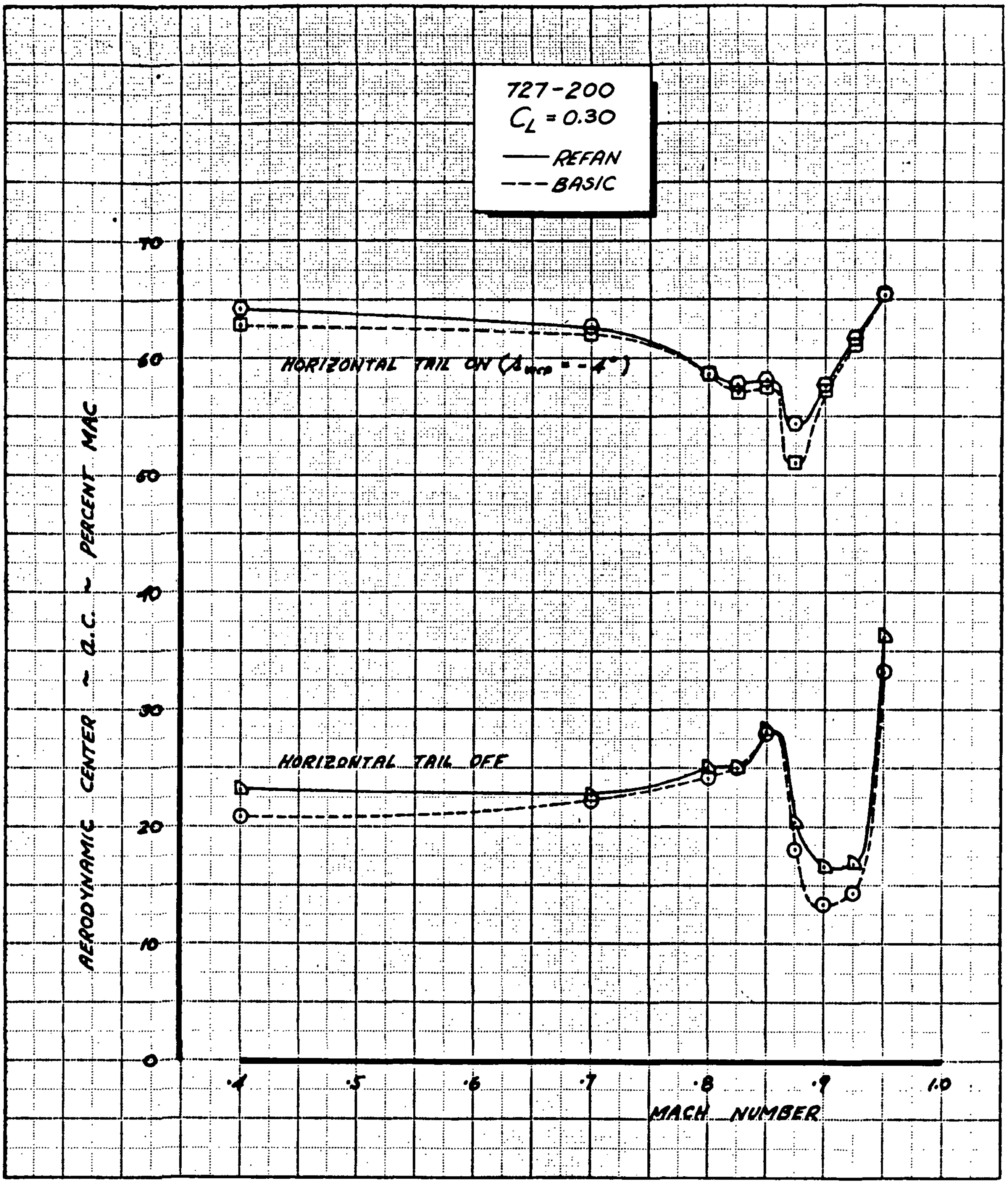

FIGURE 11. – EFFECT OF NASA REFAN NACELLES ON LONGITUDINAL STABILITY, 727-200, $C_L = 0.30$

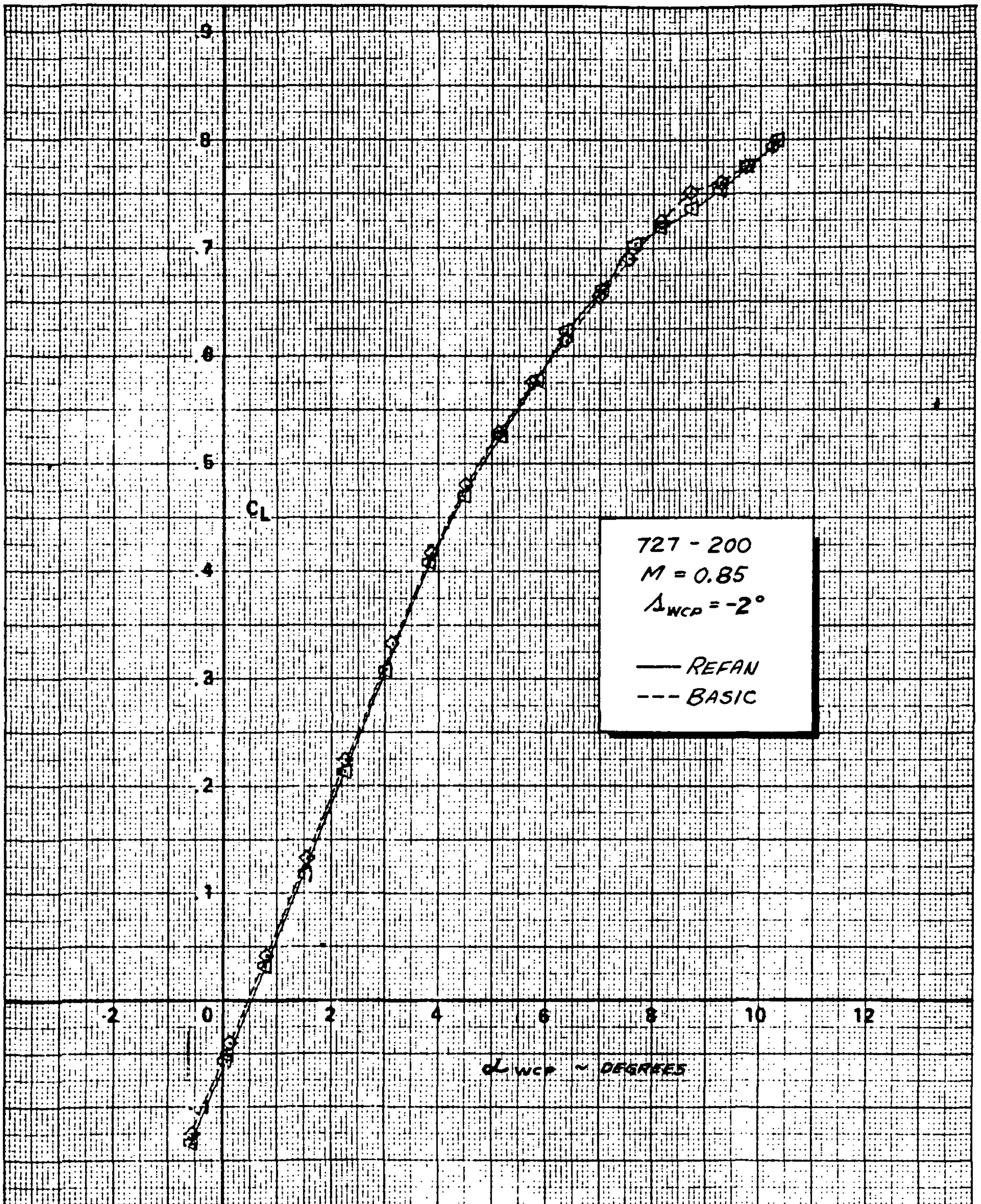

FIGURE 12.- EFFECT ON NASA REFAN NACELLES ON LIFT
727-200, M=0.85

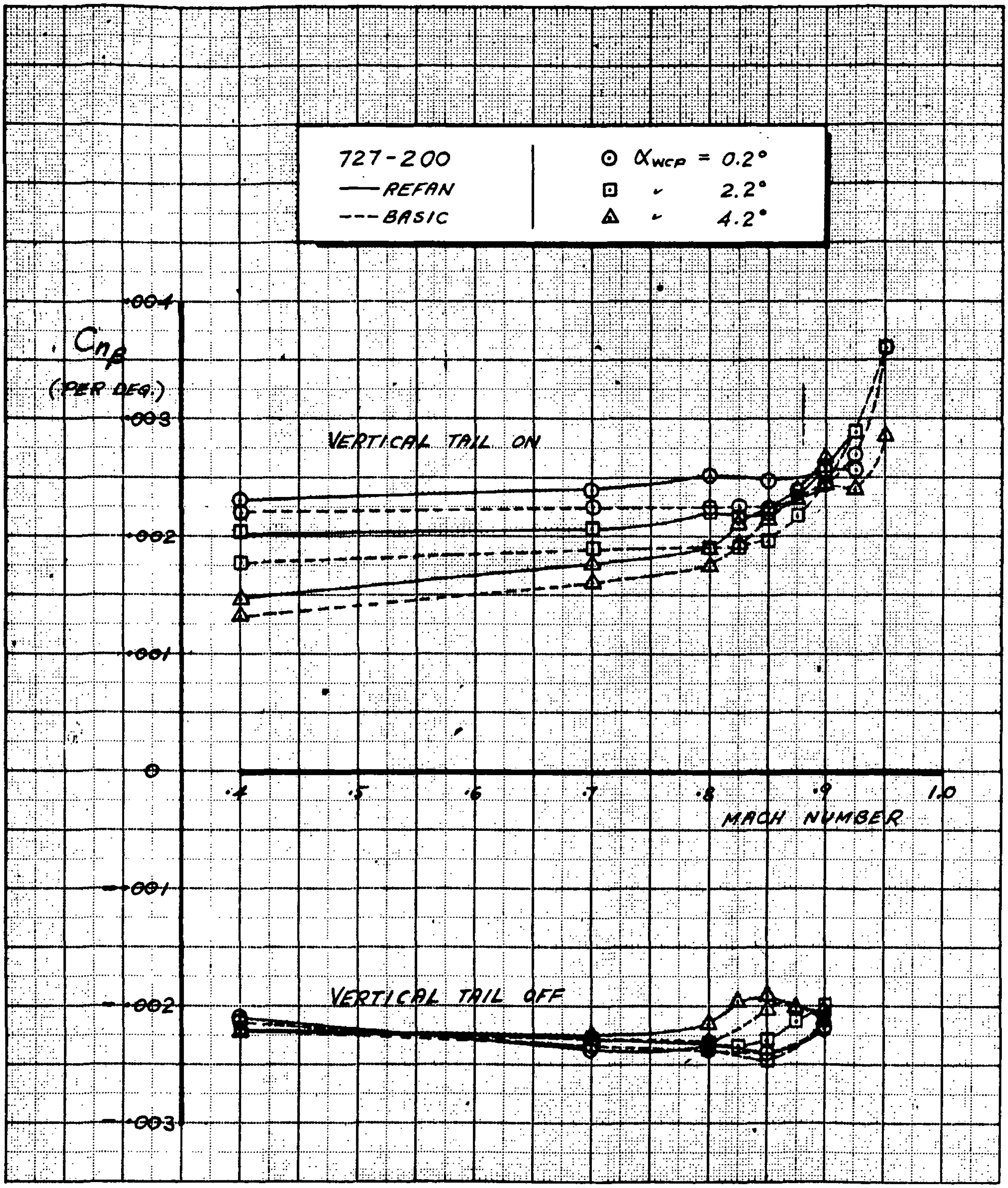

FIGURE 13. – EFFECT OF NASA REFAN NACELLES ON DIRECTIONAL STABILITY (C_{n_β}) 727-200

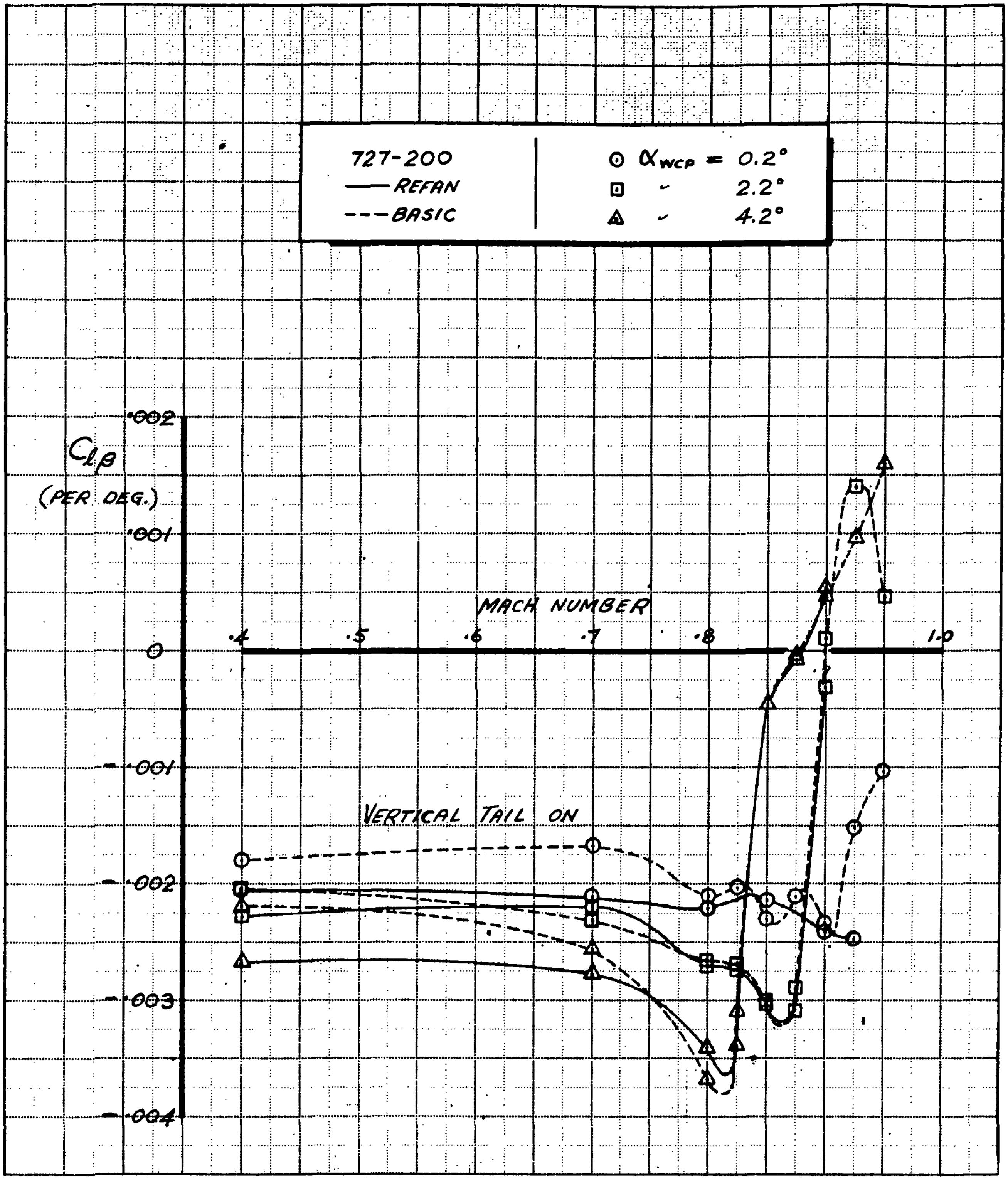

FIGURE 14. – EFFECT OF NASA REFAN NACELLES ON LATERAL STABILITY ($C_{l\beta}$)
727-200, VERTICAL TAIL ON

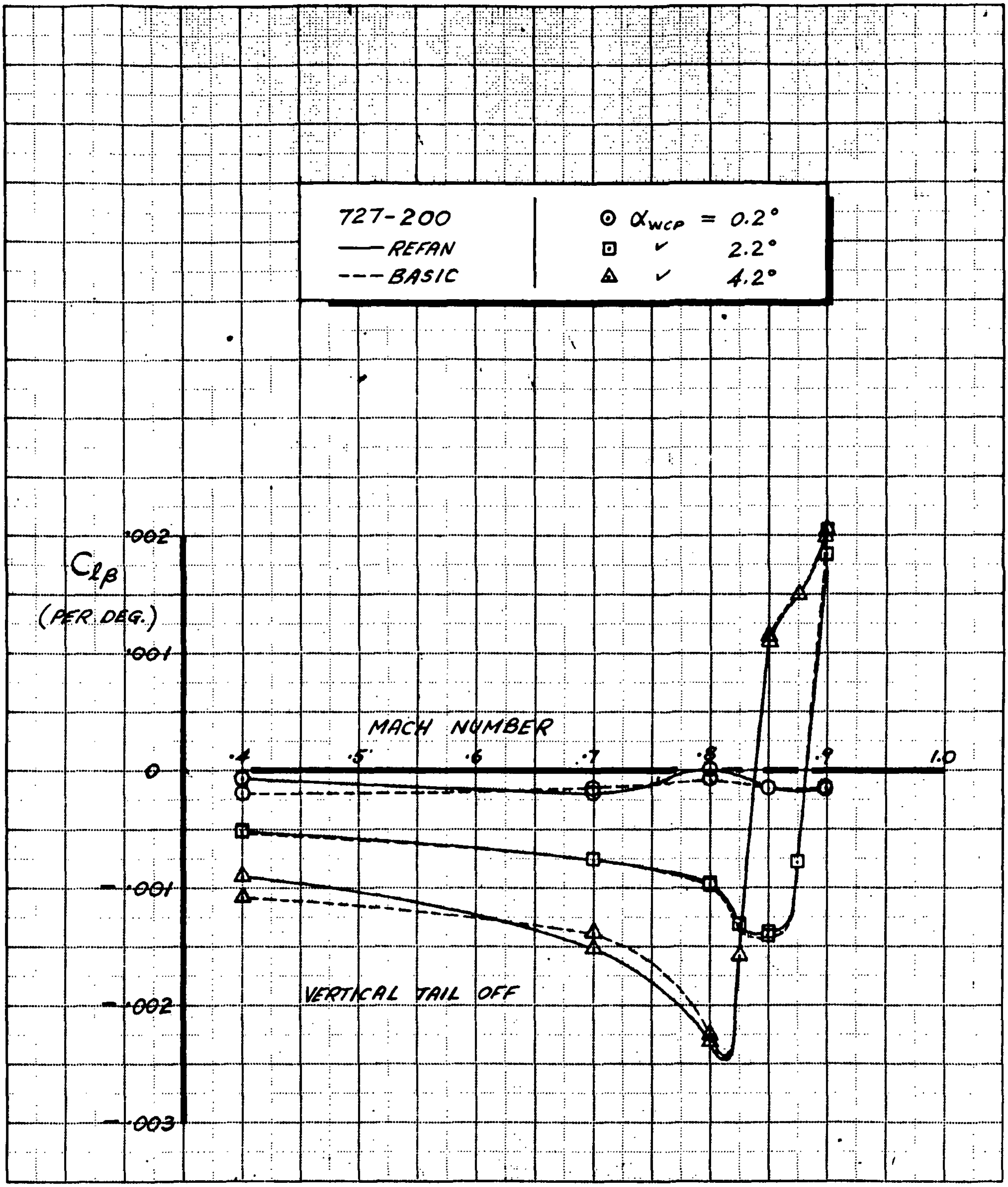

FIGURE 15. – EFFECT OF NASA REFAN NACELLES ON LATERAL STABILITY ($C_{l\beta}$)
727-200, VERTICAL TAIL OFF

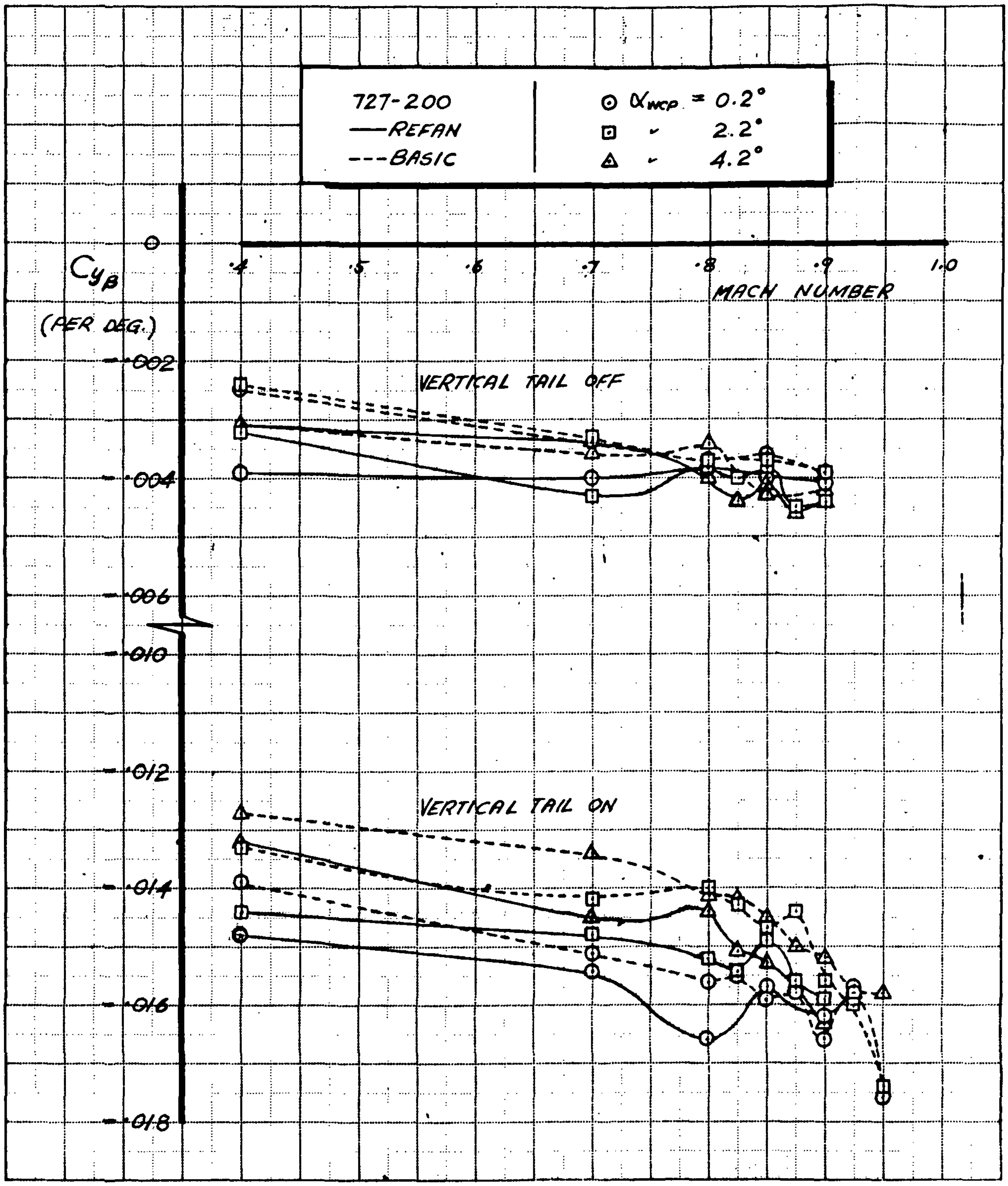

FIGURE 16. - EFFECT OF NASA REFAN NACELLES ON C_{y_β}, 727-200

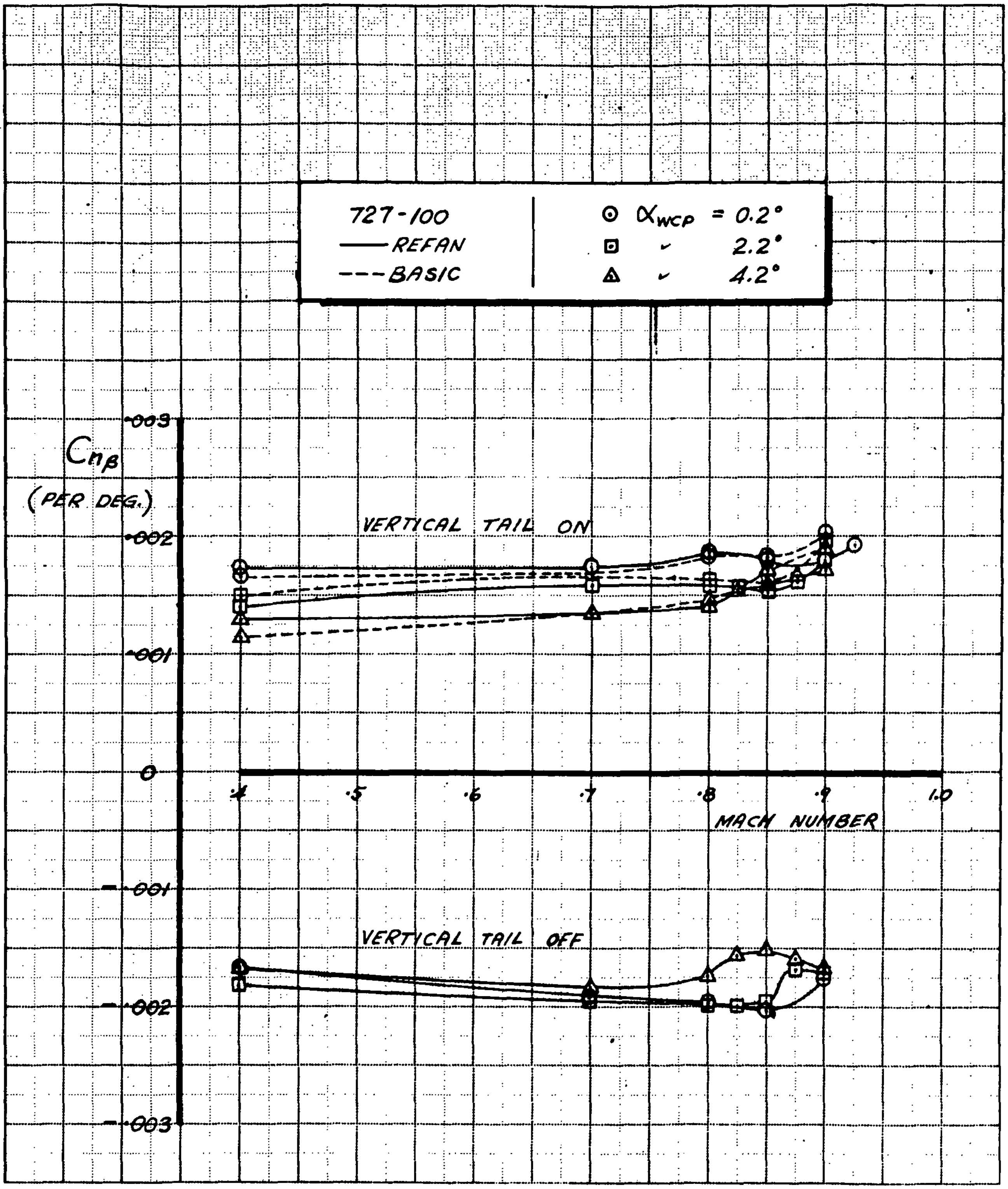

FIGURE 17. – EFFECT OF NASA REFAN NACELLES ON DIRECTIONAL STABILITY (C_{n_β}) 727-100

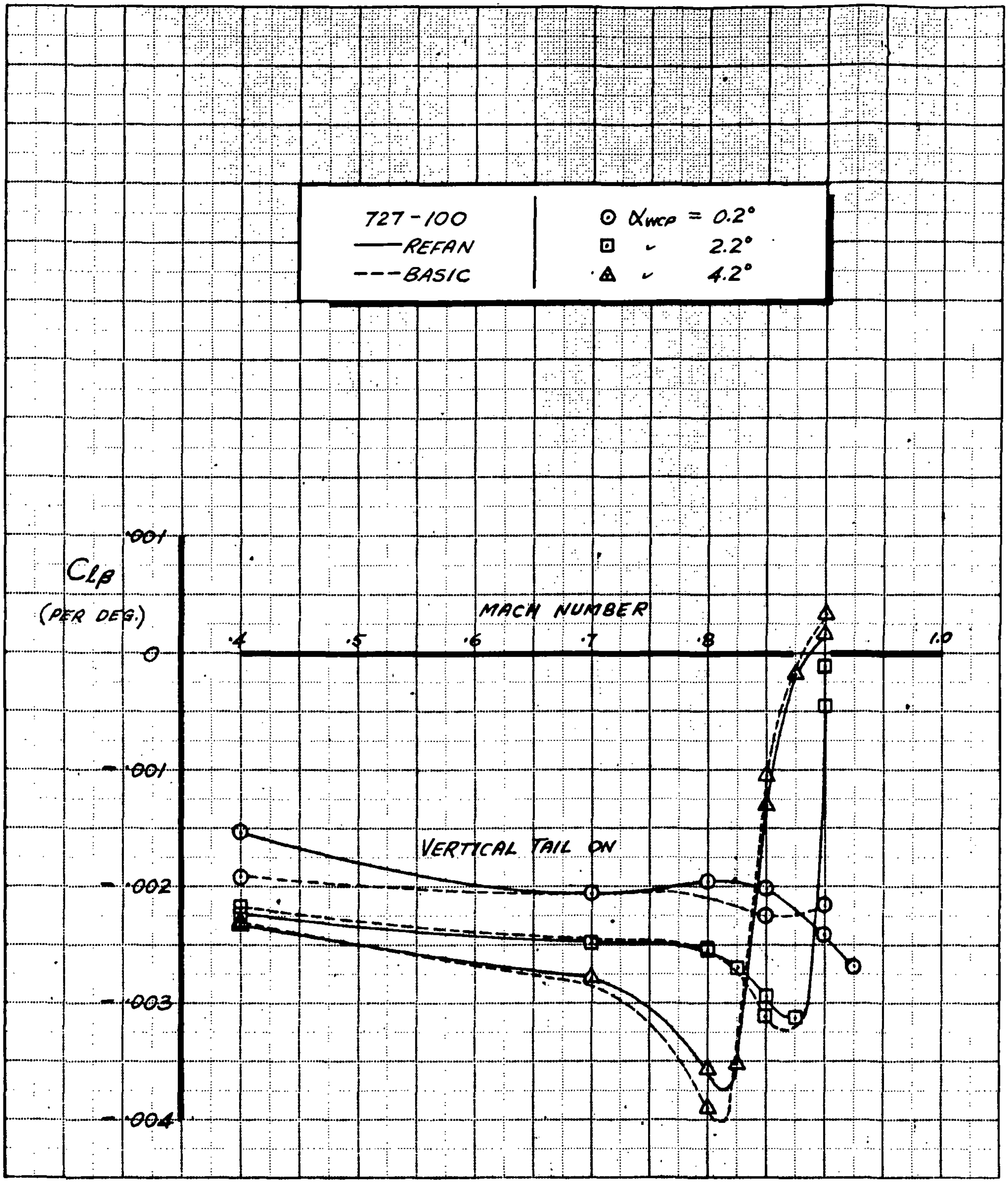

FIGURE 18. - EFFECT OF NASA REFAN NACELLES ON LATERAL STABILITY ($C_{\ell\beta}$), 727-100, VERTICAL TAIL ON

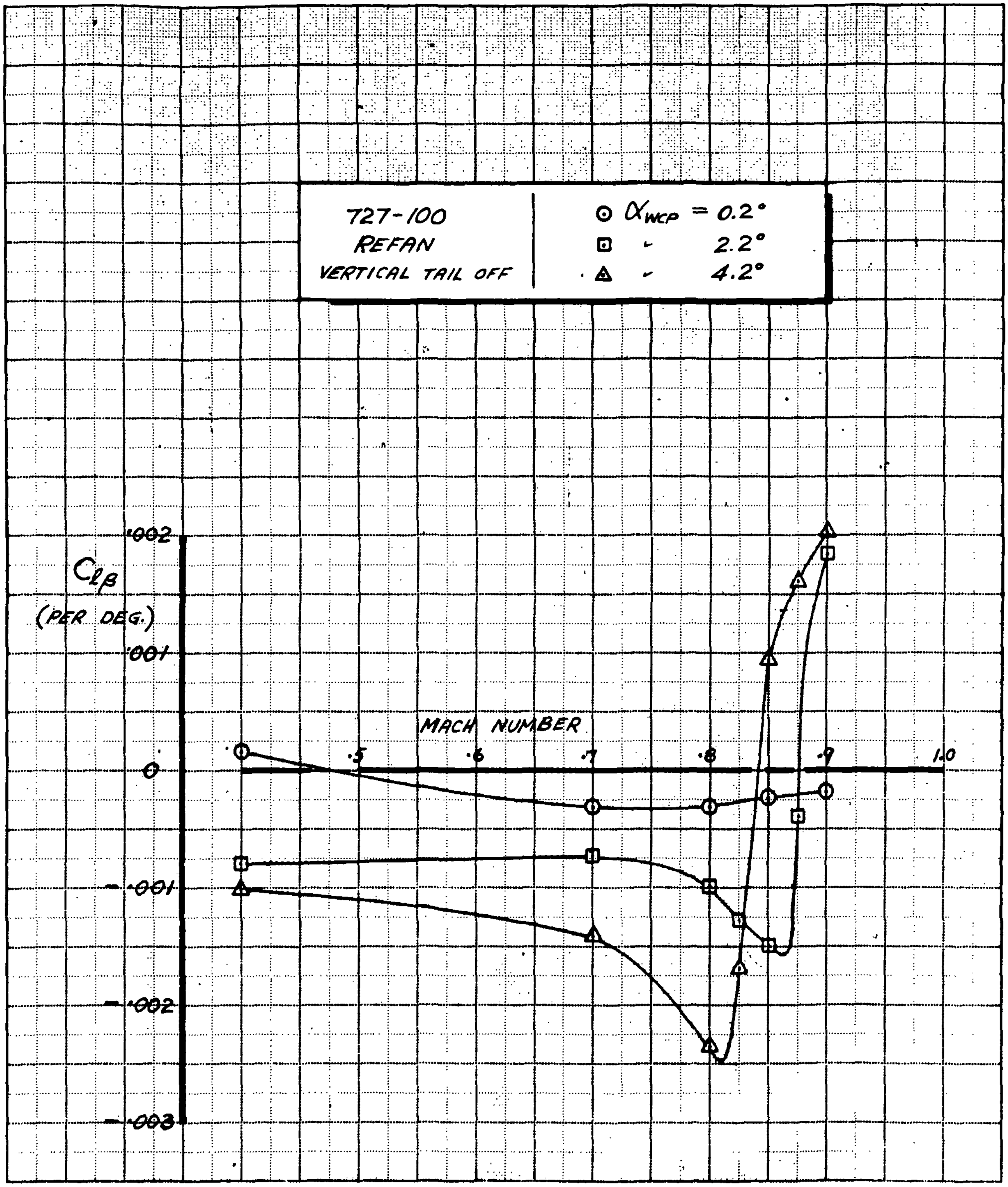

FIGURE 19. - 727-100 REFAN LATERAL STABILITY ($C_{\ell\beta}$), VERTICAL TAIL OFF

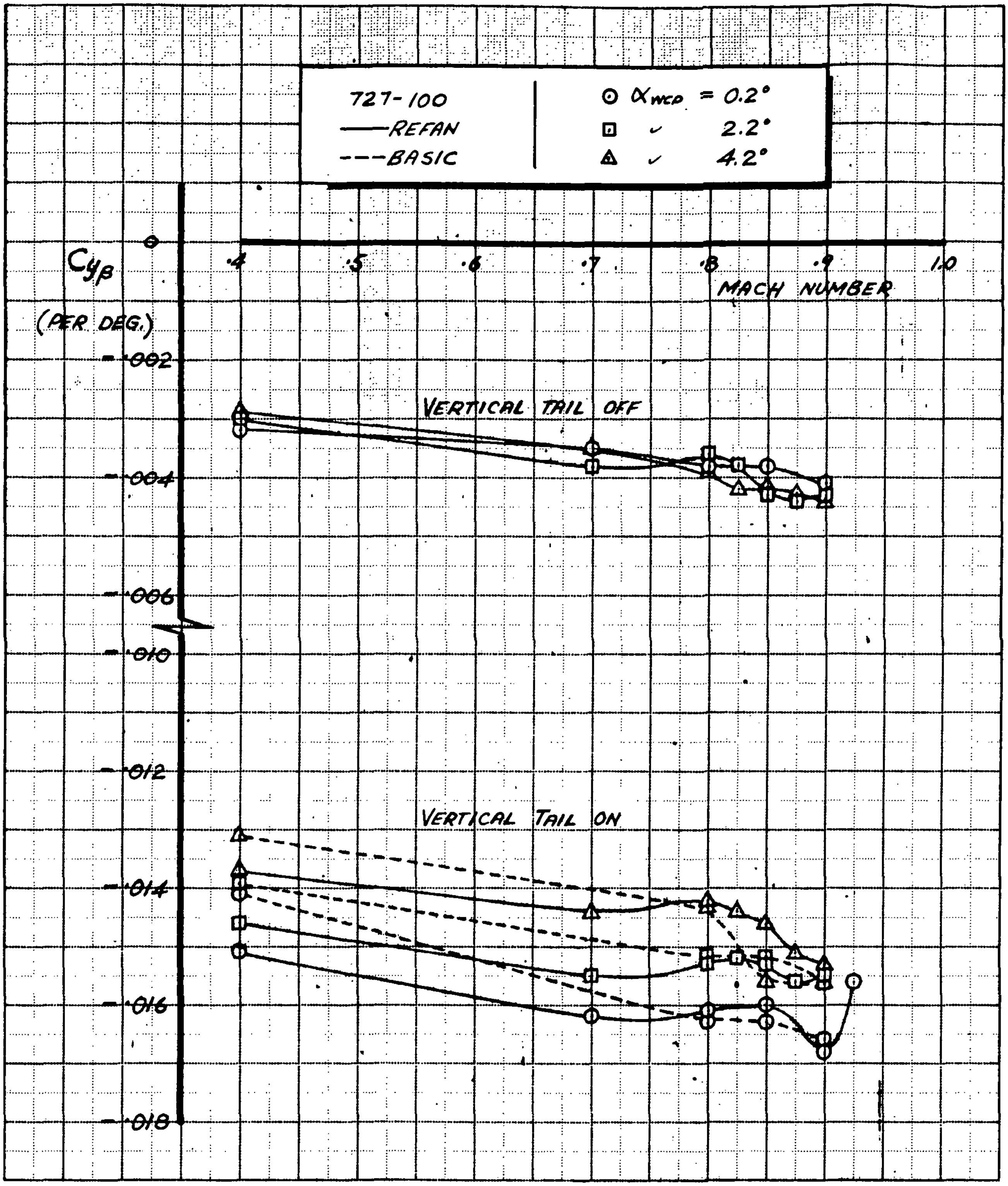

FIGURE 20.- EFFECT OF NASA REFAN NACELLES ON C_{y_β}, 727-100

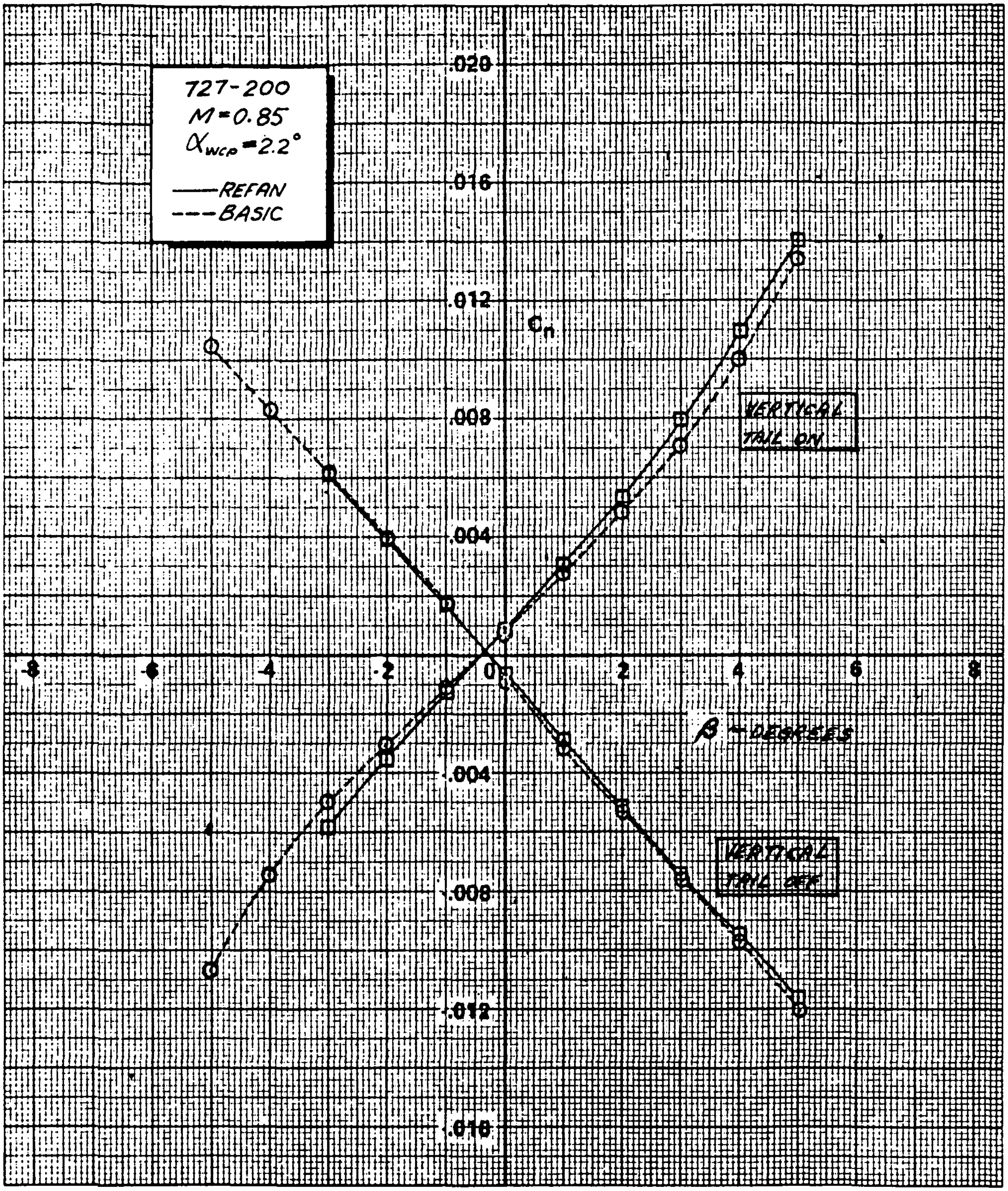

FIGURE 21. - EFFECT OF NASA REFAN NACELLES ON DIRECTIONAL STABILITY, C_n VS β, 727-200, M=0.85, α_{wcp} = 2.2°

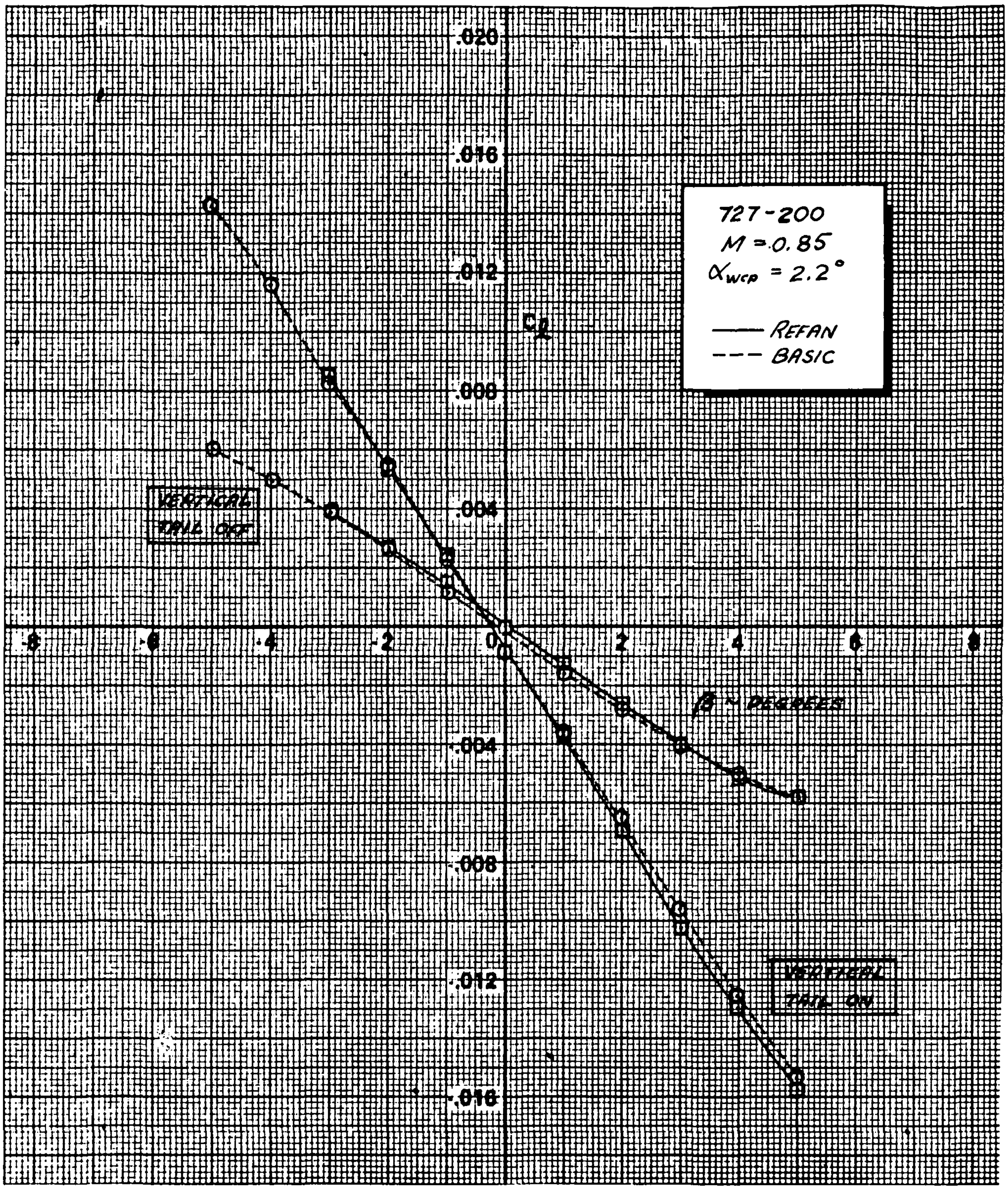

FIGURE 22. – EFFECT OF NASA REFAN NACELLES ON LATERAL STABILITY, C_ℓ VS β, 727-200, M = 0.85, α_{wcp} = 2.2°

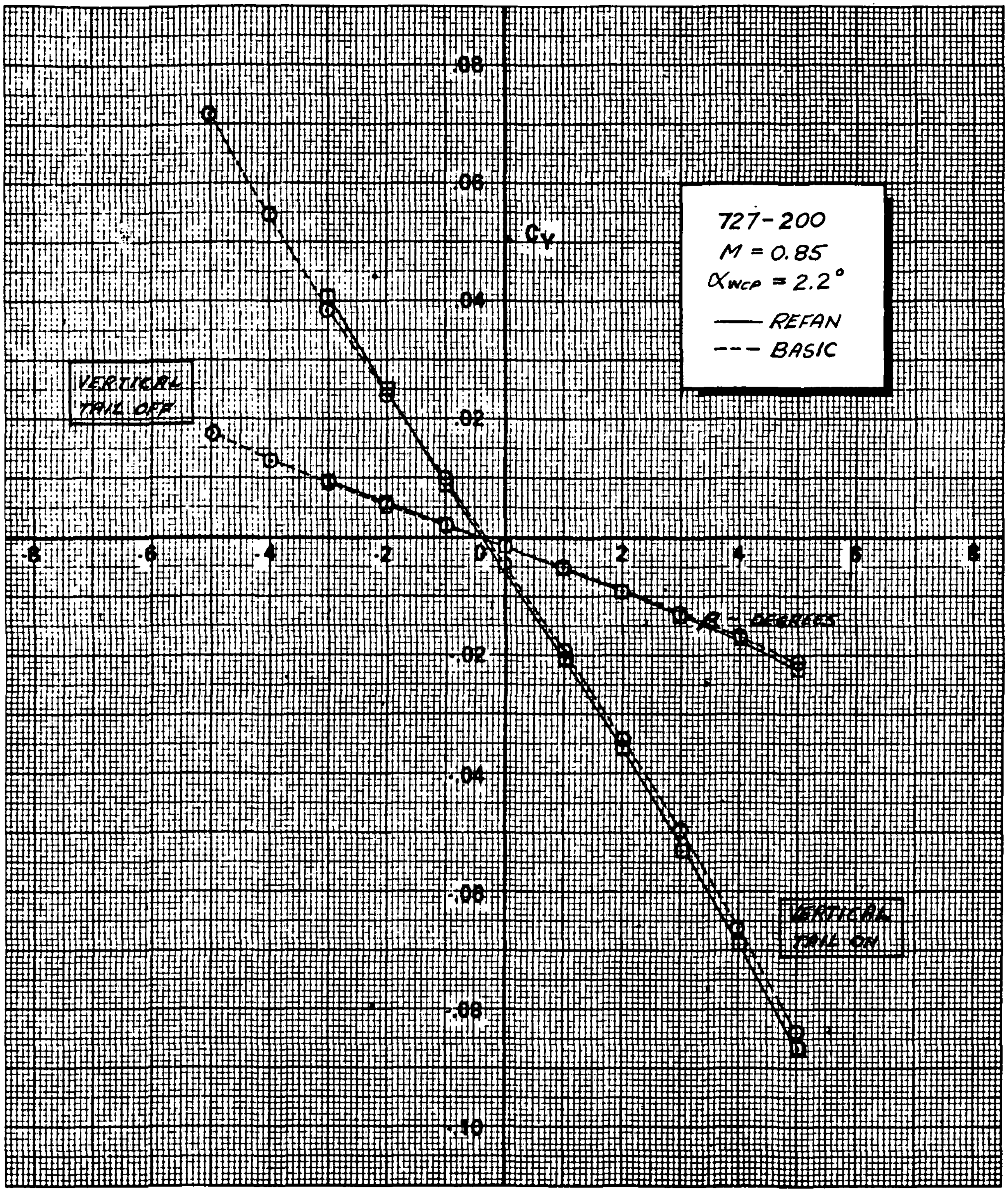

FIGURE 23. – EFFECT OF NASA REFAN NACELLES ON SIDE FORCE, C_Y VS β, 727-200, M = 0.85, α_{WCP} = 2.2°